Osteoporos Int (2016) 27:93–104
DOI 10.1007/s00198-015-3217-8

ORIGINAL ARTICLE

Alkaline biodegradable implants for osteoporotic bone defects—importance of microenvironment pH

W. Liu[1,2] · T. Wang[2] · C. Yang[3] · B. W. Darvell[4] · J. Wu[1] · K. Lin[5] · J. Chang[5] · H. Pan[2] · W. W. Lu[1]

Received: 27 April 2015 / Accepted: 16 June 2015 / Published online: 2 July 2015

Abstract
Summary Change of microenvironment pH by biodegradable implants may ameliorate unbalanced osteoporotic bone remodeling. The present work demonstrated that a weak alkaline condition stimulated osteoblasts differentiation while suppressed osteoclast generation. In vivo, implants with an alkaline microenvironment pH (monitored by a pH microelectrode) exhibited a promising healing effect for the repair of osteoporotic bone defects.
Introduction Under osteoporotic conditions, the response of the bone microenvironment to an endosseous implant is significantly impaired, and this substantially increases the risk of fracture, non-union and aseptic implant loosening. Acid-base equilibrium is an important factor influencing bone cell behaviour. The present purpose was to study the effect of a series of alkaline biodegradable implant materials on regeneration of osteoporotic bone defect, monitoring the microenvironment pH (με-pH) over time.
Methods The proliferation and differentiation potential of osteoporotic rat bone marrow stromal cells and RAW 264.7 cells were examined under various pH conditions. Ovariectomized rat bone defects were filled with specific biodegradable materials, and με-pH was measured by pH microelectrode. New osteoid and tartrate-resistant acid phosphatase-positive osteoclast-like cells were examined by Goldner's trichrome and TRAP staining, respectively. The intermediate layer between implants and new bone were studied using energy-dispersive X-ray spectroscopy (EDX) linear scanning.
Results In vitro, weak alkaline conditions stimulated osteoporotic rat bone marrow stromal cells (oBMSC) differentiation, while inhibiting the formation of osteoclasts. In vivo, με-pH differs from that of the homogeneous peripheral blood and exhibits variations over time particular to each material. Higher initial με-pH was associated with more new bone formation, late response of TRAP-positive osteoclast-like cells and the development of an intermediate 'apatitic' layer in vivo. EDX suggested that residual material may influence με-pH even 9 weeks post-surgery.
Conclusion The pH microelectrode is suitable for in vivo με-pH detection. Alkaline biodegradable materials generate an in vivo microenvironmental pH which is higher than the normal physiological value and show promising healing effects in the context of osteoporotic bone defects.

Keywords Bone remodeling · In vivo microenvironment pH · Orthopaedic biomaterials · Osteoporotic bone defect

Wenlong Liu, Ting Wang and Chun Yang contributed equally to this work.

Electronic supplementary material The online version of this article (doi:10.1007/s00198-015-3217-8) contains supplementary material, which is available to authorized users.

✉ H. Pan
hb.pan@siat.ac.cn

✉ W. W. Lu
wwlu@hku.hk

[1] Department of Orthopaedics and Traumatology, Faculty of Medicine, The University of Hong Kong, Pokfulam, Hong Kong

[2] Shenzhen Key Laboratory of Marine Biomedical Materials, Shenzhen Institutes of Advanced Technology, Chinese Academy of Sciences, Shenzhen, China

[3] School of Medicine, Shenzhen University, Shenzhen 518052, China

[4] Dental Materials Science, Department of Bioclinical Sciences, Faculty of Dentistry, Kuwait University, Kuwait City, Kuwait

[5] State Key Laboratory of High Performance Ceramics and Superfine Microstructure, Shanghai Institute of Ceramics, Chinese Academy of Sciences, Shanghai, China

Introduction

Osteoporosis is a disease characterized by low bone mass with deterioration of bone microstructure; it leads to nearly 9 million fractures annually worldwide [1]. In osteoporotic bone, the unbalanced activity of osteoblasts and osteoclasts generates a hostile microenvironment, which in turn causes the continuous loss of bone mineral [2]. The risk of fracture, non-union and aseptic implant loosening is significantly increased for osteoporotic fracture patients due to the impaired response of the bone microenvironment to the endosseous implant material. However, there are no materials specifically tailored for application in osteoporotic bone [3], although several reports have advocated combining fracture treatment with pharmaceutical therapies and claimed promising effects in preventing secondary fractures in postmenopausal women [4, 5].

Current pharmaceutical therapies for osteoporosis appear to rely on modulating the communication between osteoblasts and osteoclasts, generally by focusing on one or the other, while ignoring their microenvironment. In this context, implants generate their own milieu through biodegradation, and this may influence the regeneration of osteoporotic bone. That is, control of this might be used to influence favourably the bone remodeling microenvironment.

Within that microenvironment, the acid-base balance is important for the remodeling process and the interaction between osteoblast and osteoclast [6]. Clinically, systemic metabolic acidosis causes calcium efflux, inhibits bone formation and stimulates resorption [6, 7]. Conversely, alkalosis decreases bone calcium efflux [8]. Also, it has been postulated that a relatively high local pH is necessary during the bone formation process [9] since alkaline phosphatase (ALP) activity increases at pH 8.5 in comparison with the nominal 'physiological' value of 7.4 [10].

Previously, we have demonstrated that the pH at the surface of a material is different from that of a homogeneous bulk extract at an early stage in vitro and that the altered local pH affects significantly the proliferation and ALP activity of osteoblasts [11]. Shen et al. considered that the weakly alkaline surface pH of borosilicate shows the potential to stimulate osteoblast viability and activity, thus further facilitating apatite nucleation [12]. Another example is the spontaneous formation of an apatitic layer on the surface of 45S5 Bioglass [13]; this may also be related to the release of alkaline ions, which drive the nucleation of the apatitic material by raising the local pH. However, the usual simple extraction method [14, 15] is not suitable for examining the effect of a material's microenvironment pH (μe-pH) in vivo, since a cascade of tissue responses on the implant surface (e.g. plasma protein binding, coagulation, immune response) [16, 17] may affect the μe-pH variation caused by biodegradation. Also, blood and tissue fluid perfusion may offset or neutralize such μe-pH changes in vivo. Therefore, direct detection and long-term observation of the orthopaedic implanted material's in vivo μe-pH is an important objective.

It has been said to be difficult to evaluate rapidly μe-pH near the surface of implants in vivo [18]. The techniques used for pH detection in vivo are of three kinds [19]: electrochemical (e.g. convention glass pH electrode [20]), gravimetric [21] and spectroscopic (e.g. nuclear magnetic resonance (NMR)-based spectroscopy [22]; near-infrared diffuse reflectance spectroscopy (NIRS) [23]). However, the ordinary bulky glass pH electrode is not suitable for measuring μe-pH, the gravimetric pH detection system has the drawback of a long response time, while NMR cannot be used routinely [19]. In addition, pH detection based on fluorescence ratio imaging microscopy is susceptible to photobleaching (variation in light scattering and adsorption of the sample are other drawbacks), but also, the interaction of pH indicators with intracellular proteins may change the fluorescence intensity ratio [24]. In a recent study, the optical detection of local pH in a subcutaneous region indirectly but non-invasively was based on a fluorophore, 5-(and-6)-carboxy SNARF-1 [25]. However, due to its low sensitivity, the result is far from satisfactory. Earlier, using a pH microelectrode, Chakkalakal et al. detected tissue pH changes during the bone healing process and concluded that the pH of repair tissue fluids may play a regulatory role in bone healing and the mineralization process [26]. Overall, knowledge of material μe-pH change after implantation remains sketchy.

The present study was to use pH microelectrodes to monitor the μe-pH for various materials at the implant site spatiotemporally. A series of alkaline biodegradable implants were designed to modulate the bone remodeling process under osteoporotic conditions and intended to generate higher values of μe-pH than those obtained in the 'blank' control defect. β-Tricalcium phosphate (β-TCP) is a well-studied and widely used orthopaedic biodegradable material, while biodegradable calcium silicate (CS) has been investigated as it has shown promising 'bioactivity' [27]. Compared with β-TCP, CS generates a higher μe-pH value as silicic acid is weaker than phosphoric acid. Ten per cent strontium-substituted calcium silicate (Sr-CS) generates a yet higher μe-pH than CS [8] because Sr^{2+} is a relatively stronger alkali ion in comparison with Ca^{2+}. Tissue responses under such altered pH conditions were then investigated.

Materials and methods

Implant materials

Powdered samples of β-tricalcium phosphate (β-TCP), calcium silicate (CS) and 10 % strontium-substituted calcium silicate (Sr-CS) were kindly provided by Shanghai Institute of Ceramics, Chinese Academy of Sciences. Briefly, material powders were synthesized by a chemical precipitation method

as previously described [27] and then had been sieved to the size range 300–450 μm. The nature of all materials used in this study was confirmed by FTIR spectrophotometry (data not shown). All materials were sterilized by gamma irradiation (270 Gy) before use.

In vitro cell culture

Preparation of oBMSCs and cell culture

Osteoporotic rat bone marrow stromal cells (oBMSCs) were extracted from the established osteoporotic model using the methods previously described [28]. The oBMSCs were cultured in minimum essential medium eagle alpha modification (α-MEM) with 10 % fetal bovine serum (FBS, Biosera, Kansas City, MO, USA), sodium bicarbonate (23.8 mM), HEPEs (22.3 mM), 1 % penicillin (10^4 units/mL), streptomycin (10^4 μg/mL) (P/S, Gibco), 2 mmol/L-glutamine (Gibco) and 1 μg/mL Amphotericin B (Fungizone, Gibco), at 37 °C in a 5 % CO_2 incubator. The medium was changed every 2–3 days. The extracted oBMSCs were confirmed to have the capability of differentiating into osteoblasts, chondrocytes and adipocytes (data not shown).

A material 'extract' was prepared by immersing Sr-CS particles in α-MEM for 24 h (200 mg/mL), and the retrieved supernatant diluted 1:16. The pH of aliquants of the media (α-MEM, 'α', or Dulbecco's modified Eagle's medium (DMEM), 'D') was then adjusted by adding 2.5 % (*v*/*v*) of the following solutions 0.5 and 1 mol/L HCl; H_2O (control); 0.5, 1 and 2 mol/L NaOH and allowed to equilibrate under culture conditions overnight. The pH values were then recorded. The pH-adjusted media were used to culture oBMSCs (α-MEM) or RAW 264.7 cells (DMEM). Adjusted media were expressed as follows: −− (1 mol/L HCl), − (0.5 mol/L HCl), 0 (H_2O), + (0.5 mol/L NaOH), ++ (1 mol/L NaOH) and +++ (2 mol/L NaOH); the relevant culture condition code is then indicated as, for example: 'α^{++}' (see Supplement Table 1).

oBMSC proliferation and differentiation activity

The oBMSCs were seeded in 96-well plates with an initial density of 10^4 cells/mL and 100 μL per well in α-MEM with 10 % FBS. After 12 h, the medium was replaced by one of the pH-adjusted culture media and this was then changed every 3 days. 3-(4,5-Dimethylthiazol-2-yl)-2,5-diphenyltetrazolium bromide (MTT) assays were conducted as previous described [12] at 1, 3 and 5 days. The OD values at 570 and 650 nm were recorded by microplate reader (n=4) (Multiskan Go, Thermo Scientific, West Palm Beach, FL, USA) and expressed as $\Delta OD = OD_{650} - OD_{570}$.

For ALP assay, the oBMSCs were seeded in a 96-well plate with an initial density of 5×10^4 cells/mL and 100 μL per well. The culture medium (osteogenesis medium, 'O') was supplemented with 10 mM β-glycerophosphate disodium salt pentahydrate (MP Biomedicals, Santa Ana, CA, USA), 10 nM dexamethasone (Sigma–Aldrich) and 50 μg/mL L-ascorbic acid 2-phosphate sesquimagnesium salt hydrate (Sigma–Aldrich). After 7 days, ALP activity was quantified by previously described procedures [11], while total protein content was measured by Pierce BCA Protein Assay Kit following manufacturer's instruction (Thermo Scientific). ALP activity was expressed as rate of *p*-nitrophenol production (μmol mL^{-1} mg^{-1} h^{-1}).

Osteoclast formation capability

The influence of altered μe-pH on osteoclasts was also examined in vitro. A mouse leukaemic monocyte macrophage cell line (RAW 264.7; ATCC, Manassas, VA, USA) was used for osteoclast precursors. Cells were seeded in a 96-well plate with an initial density of 10^4 cells/mL in 100 μL and cultured in DMEM with 10 % FBS, supplemented with 35 ng/mL receptor activator of nuclear factor κB ligand (RANKL) (R and D Systems, Minneapolis, MN, USA). After 5 days' culture, cells were washed with PBS. The osteoclast formation capability was quantified by measuring the area of TRAP-positive multinucleate osteoclasts using a leukocyte acid phosphatase kit (Sigma–Aldrich). Images were captured by microscope in which the area of fused multinucleated TRAP-positive osteoclasts was calculated in software (Image-Pro Plus). The proliferation rate under the various pH-adjusted conditions was also checked by the MTT method described before (Section 2.2.2).

Animal model

All animal surgical procedures were performed under protocols approved by the Committee on the Use of Live Animals in Teaching and Research, The University of Hong Kong (CULATR No. 2572–11; 2555–11).

Osteoporotic rat model

Ovariectomy (OVX) was performed on 42 female Sprague-Dawley rats of age between 10 and 11 months, as previously described [29, 30]. Bone mineral density (BMD) of spongy bone at the metaphysis of both tibiae was evaluated twice monthly using computed microtomography (in vivo X-ray microtomograph) (Skyscan 1076, Skyscan, Kontich, Belgium). At 3 months post-OVX, the osteoporotic rat models were successfully established.

Material implantation

At 3 months post-OVX, secondary surgery was performed to establish bone defects bilaterally in the

median aspect of the tibial shaft, below the tibial plateau. Briefly, after routine shaving and aseptic procedures, an incision was made to expose the bone, and a defect (depth ~3 mm, diameter ~3 mm) was created with a 3-mm drill at low speed without irrigation. Both defects were then packed gently with one of the test powders. Each material had four replicates for each time point examined. After μe-pH measurement (Section 2.4), the entrance of the defect was sealed using bone wax (Ethicon, Somerville, NJ, USA) and the skin sutured (Ethilon, Ethicon,). Blank controls were treated similarly but without material implantation. Antibiotic (Enrofloxacin, Bayer HealthCare, Kiel, Germany) was administered in the drinking water provided ad libitum as a post-operative antibiotic for 3 days (estimated total dose: 5 mg/kg). Euthanasia with an overdose of pentobarbital (Alfasan) (150 mg/kg) was performed at 3 days and at 1, 4 and 9 weeks. Both tibiae were then harvested, along with the femurs for cell culture use (Section 2.1).

In vivo μe-pH

The μe-pH was determined immediately after implantation using a pH meter (Model 60, Jenco, San Diego, CA, USA). The sensing tip of the microelectrode (MI-413P, Microelectrodes, Bedford, NH, USA) was placed on the surface of the blood-saturated packed powder at three random locations. The average of the stable values was used for analysis. Protein contamination on the sensor was removed after each measurement by immersing the sensor in enzymatic detergent (1 % solution; Tergazyme, Alconox, White Plains, NY, USA) for approximately 2 min at room temperature (and for 30 min after each session) and then rinsing with deionized water. If the electrode response became slow, it was replaced. Before tissue was harvested, the bone wax was removed, and the surface layers of the implants were carefully scraped with a scalpel to expose the implant fully and thus its internal microenvironment, for its μe-pH to be measured again in the same way. The systemic homogeneous pH of peripheral blood was measured by microelectrode at muscle near the surgical site at each time point.

Evaluation of bone defect

Micro-CT analysis

Micro-computerized tomography (CT) (Skyscan 1076) was used to assess the response to and behaviour of each test material, scanning implantation sites at 88 kV (pixel size, 18 μm). The data were reconstructed in software (NRecon Server, version 1.6.6.0, Skyscan). A column 0.4×1.0 mm^2 (height × radius) in the centre of the implantation site was chosen as the volume of interest (VOI). The 3D VOI images at each time point were created based on attenuate coefficient (AC) (CT Vol, version 2.1.0.0, Skyscan).

H&E and TRAP staining

Five-micrometer paraffin-embedded decalcified sections were prepared using standard procedures [31] and were used for haematoxylin and eosin staining (Sigma–Aldrich) to detect the specific tissue response to the implanted materials.

The activity of tartrate-resistant acid phosphatase (TRAP)-positive osteoclast-like cells was determined using an acid phosphatase, leukocyte kit (Cat. No. 387a, Sigma–Aldrich). Care was taken to avoid identifying macrophages (by location and morphology; Fig. 4), which can also express TRAP [32], as osteoclast-like cells. Images were captured by microscope (Eclipse 80i, Nikon, Tokyo, Japan). The new bone volume/tissue volume ratio (V_{NB}/V_T) was calculated semi-quantitatively (n=8).

Goldner's trichrome and toluidine blue staining

To check osteoblasts' new osteoid formation capability, 50-μm undecalcified sections were prepared using Exakt system (model 310 CP band system, Exakt, Oklahoma City, OK, USA) and were stained with Goldner's trichrome at 4 and 9 weeks. Toluidine blue staining (at 1, 4 and 9 weeks) was used to distinguish better the boundary between the implant and new bone. All processing and staining procedures were conducted according to standard protocol [31].

Elemental analysis

An energy-dispersive X-ray spectroscopy (EDX) detector (EMAX, EX-350, Horiba, Tokyo, Japan) on a scanning electron microscope (S-4800 FEG, Hitachi, Tokyo, Japan) was used to assess elemental distribution development over time. Sections of 200-μm thickness were carbon-sputtered (Polaron E6700, Quorum Technologies, Newhaven, East Sussex, UK). The distribution of Ca, P and Si was recorded in linear scan mode at an operating voltage of 20 kV. Data were analysed in software (INCA Energy software, Oxford Instruments, Abingdon, Oxfordshire, UK).

Statistical analysis

Quantitative results were expressed as the mean±standard deviation (SD). All statistical analyses were performed in software (SPSS Statistics for Windows 17.0, SPSS, Chicago, IL, USA; SigmaPlot 12.5, Systat Software, San Jose, CA, USA; Mathematica 9, Wolfram Research, Champaign, IL, USA). The critical value was set at α=0.05.

Results

Extracellular pH

The adjusted pH values of the various culture media are listed in Supplementary Table 1. As shown in Fig. 1a, the proliferation of oBMSCs was significantly inhibited when the cells were cultured in either a higher or a lower pH condition than the control 'normal' α-MEM (pH 7.40±0.06), α^0. In particular, and against our previous prediction, the more alkaline conditions (α^+, α^{++}: pH 7.60~7.98) showed no positive effect on oBMSC proliferation (Fig. 1a). The alkaline-adjusted osteogenesis medium with Sr-CS extract (Supplementary Table 1; O^{++} and O^{+++}: pH 7.57~7.73) showed significantly higher ALP activity in comparison with the control group O^0 (Fig. 1b; 1 week). Qualitatively, more ALP-positive cells were observed in 10-day ALP staining in groups within this higher pH condition (Supplementary Fig. 1, pH 7.57~7.73).

According to Fig. 1c, for RAW 264.7 cells, osteoclast precursor proliferation would be optimal around pH 7.4, significantly better than for the neighbouring values tested. After RANKL treatment for 5 days, the multinucleate mature osteoclasts were stained red-purple. With increasing culture medium pH, the proliferation of osteoclast precursors was suppressed, and TRAP-positive osteoclasts appeared smaller in size (Fig. 1e) and with decreased osteoclast formation capability (D^+: 49 % inhibited; D^{++}: 65 % inhibited) which vanished in the extreme alkaline condition (D^{+++}, pH 8.00± 0.04). Notably, for D^- (pH 7.07±0.06), the differentiation of TRAP-positive osteoclasts increased significantly, though the proliferation of RAW 264.7 precursors was not as strong as in the normal pH condition. The total TRAP-positive osteoclast area was significantly negatively correlated with medium pH (r^2=0.9867, $F_{1,3}$=222.843, P=0.00065) (Fig. 1d).

μe-pH variation in vivo

As shown in Fig. 2, the peripheral blood pH values were similar at all time points and were close to those of the blank bone environment, in which no significant change was observed (7.42~7.49).

After implantation, in vivo μe-pH for β-TCP, CS and Sr-CS increased immediately in comparison with the blank group (7.42±0.02), with CS (8.17±0.06) and Sr-CS (9.16±0.11) giving a significantly higher value compared with β-TCP (7.77±0.15) (P<0.01), that is Sr-CS>CS>β-TCP (Fig. 2). The significant elevation of μe-pH persisted to day 3 (P<0.05), but had faded by 9 weeks.

The μe-pH values for β-TCP, CS and Sr-CS were generally significantly higher than for the blank, while for Sr-CS, it was higher than for CS at all time points (Fig. 2). For each material, the μe-pH dropped from the initial value at implantation to a minimum: 7.68±0.09 for β-TCP at week 1, 7.44±0.08 for CS at week 4 and 7.70±0.08 for Sr-CS at week 1. The value at week 9 was higher than for the blank, with β-TCP>Sr-CS> CS (Fig. 2).

Bone formation and biomaterial degradation

The defect in the blank group remained unrepaired at 9 weeks post-surgery (Fig. 3a), while the appearance for β-TCP did not change much over time (Fig. 3b). The material degradation rates for CS and Sr-CS were apparently greater than the rate of new bone formation (Fig. 3b), and this trend was reversed after week 4. No apparent change in total object volume was observed in VOI of β-TCP (Fig. 3b), which indicate a similar bone formation and implant degradation speed of β-TCP.

All implant powders were encapsulated by fibrous tissues at 1 week after implantation (Fig. 3a; 'F'). New bone matrix (stained pale pink) could be clearly observed for β-TCP and SR at week 4 and for CS at week 9 (Fig. 3a; 'NB'). The semi-quantitative results (Fig. 3c) indicated a significant increase in new bone with time for each material (linear regression; β-TCP: $F_{1,22}$=15.19, P=0.00078; CS: $F_{1,22}$=286.9, P=4.12×10^{-14}; Sr-CS: $F_{1,22}$=284.3, P=4.56×10^{-14}), but higher initial μe-pH gave a greater volume at week 9: Sr-CS>CS>β-TCP. For the blank group, laminar bone had grown peripherally to the defect at week 4, but the centre was left unrepaired even after 9 weeks (Fig. 3a).

For β-TCP, fibrous tissue appeared at week 1 and then diminished and was gradually replaced by bone marrow (Fig. 3a; 'BM'). However, for CS and Sr-CS, although more new bone formation was observed (Fig. 3c), the inflammatory response fibroblasts were still present at 9 weeks.

Osteoid formation and TRAP-positive cells

Typical sections are shown in Fig. 4 (Goldner's trichrome), where calcified new bone regions are stained green and new osteoid red. New osteoids were formed on the surface of the implanted materials and then gradually replaced by mineralized bone. Increased osteoid areas, indicating increased osteoblast activity, were observed for the higher μe-pH materials (CS and Sr-CS) at week 4, in comparison with β-TCP. At week 9, the osteoid content for β-TCP had diminished while remained conspicuous for CS and Sr-CS. In the blank group, osteoid was detected on the periphery of the bone defect.

Osteoclast-like cells were positively stained by TRAP during the bone healing process in the blank group (Fig. 4, TRAP staining). For β-TCP, TRAP-positive osteoclast-like cells were found as early as week 1 and then reached the highest levels at week 4. In the higher μe-pH groups, a late response of TRAP-positive osteoclast-like cells was observed: none were found at week 1, appearing at 4 weeks, and could still be seen at 9 weeks.

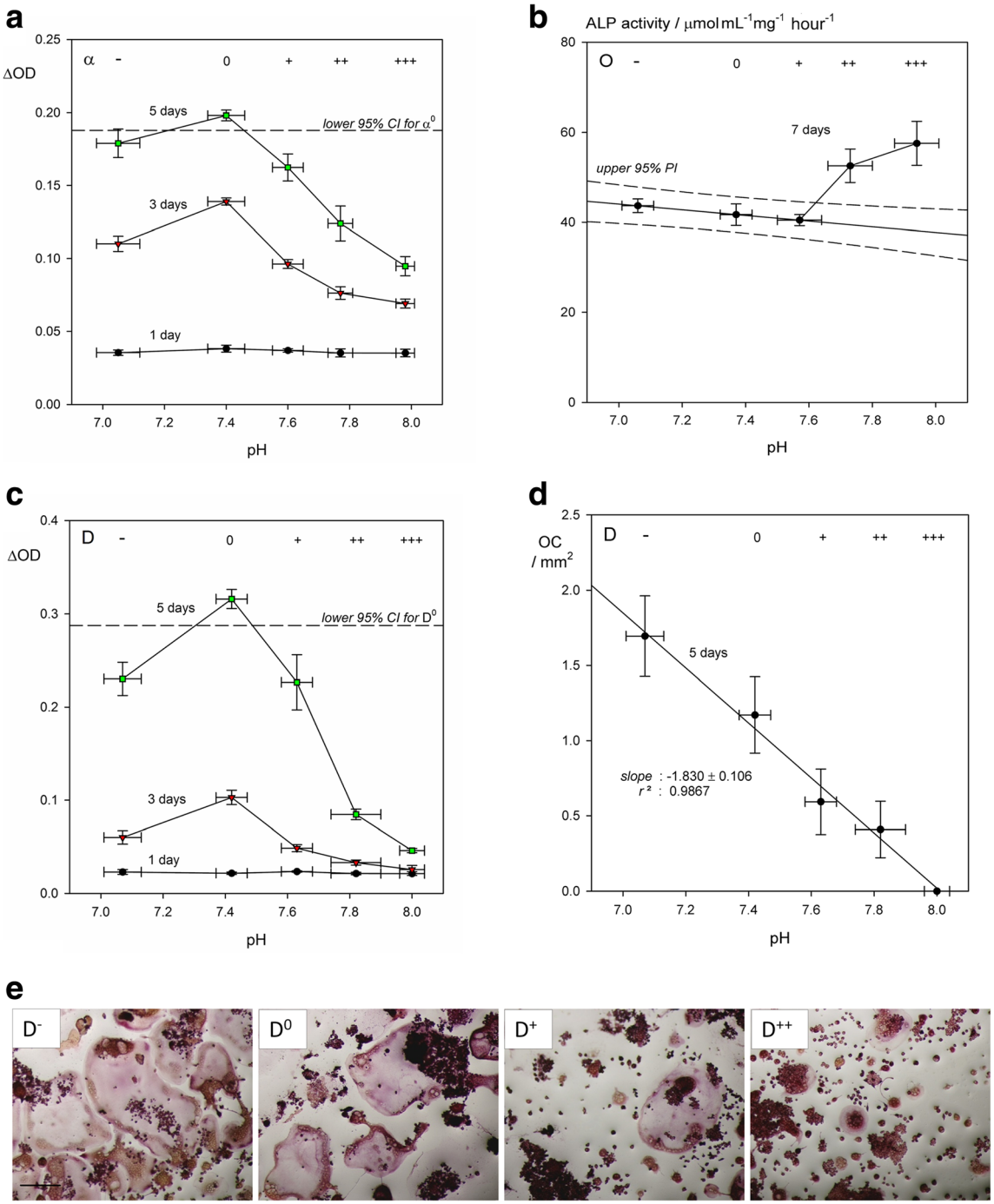

Fig. 1 Effect of culture medium pH on oBMSCs or RAW 264.7 osteoclast precursors. **a** oBMSCs proliferation in α-MEM by MTT assay (optical density difference, $\Delta OD = OD_{650} - OD_{570}$); $n=5$. **b** oBMSCs differentiation in osteogenesis medium by ALP activity in terms of rate of *p*-nitrophenol production (μmol mL^{-1} mg^{-1} h^{-1}); $n=4$; 95 % prediction interval for linear regression on −, 0 and + points shown as *dashed lines*. **c** RAW 264.7 proliferation in DMEM by MTT assay (optical density difference, $\Delta OD = OD_{650} - OD_{570}$); $n=5$. **d** Semi-quantitative image analysis for osteoclasts surface area (OC/mm^2); $n=5$. **e** TRAP staining at day 5. Multinucleate TRAP-positive osteoclasts are stained red-purple. *Scale bar* 200 μm

'Apatite' formation

Consistent with other results (Fig. 3), toluidine blue staining indicated that new bone had formed on the edge of the bone defect at weeks 4 and 9 in the blank group (Fig. 5 blank; 4 and 9 weeks). For β-TCP, particles were connected by new bone directly (Fig. 5 β-TCP; 4 and 9 weeks). A greater material degradation rate was observed in the CS and Sr-CS groups than for β-TCP. As indicated in Fig. 5, there was more new bone (NB) in the higher μe-pH conditions (CS and Sr-CS) at week 9

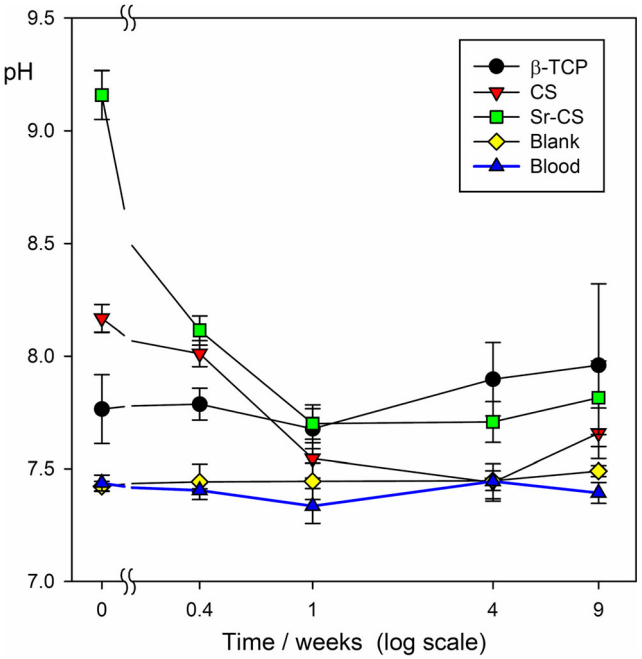

Fig. 2 Variation of μe-pH with time post-implantation. Data are expressed as the mean±standard deviation; n=4

compared with β-TCP, consistent with the H&E staining results (Fig. 3). During material degradation, an intermediate (assumed apatitic) calcium phosphate layer, but without osteocyte lacunae, was observed for CS and Sr-CS (Fig. 5). This formed as early as 1 week after Sr-CS implantation and was much larger in area than for CS. During biodegradation, the outline between material and intermediate layer became indistinct, and the 'apatitic' layer occupied most of the materials' original location (Fig. 5 CS, Sr-CS; 4 weeks). The new bone was then formed on the surface of this intermediate layer.

Residual implanted materials

Elemental distributions are shown in Fig. 6 (Ca: red, P: blue, Si: green). Silicon is the characteristic element of remaining CS and Sr-CS. Regions of new bone, remaining β-TCP particles and the intermediate layer were rich in calcium and phosphorus. Osteocyte lacunae are found only in new bone. The boundaries between materials, intermediate layers and new bone are marked with broken yellow lines. The formation of an intermediate layer was further confirmed by EDX. Si-rich regions were gradually replaced by P-rich deposition (Fig. 6 CS; 4 and 9 weeks). For β-TCP, new bone was attached to its surface directly. The original Si-rich material powder was still detectable at 9 weeks (Fig. 6 CS, Sr-CS; denoted by an asterisk).

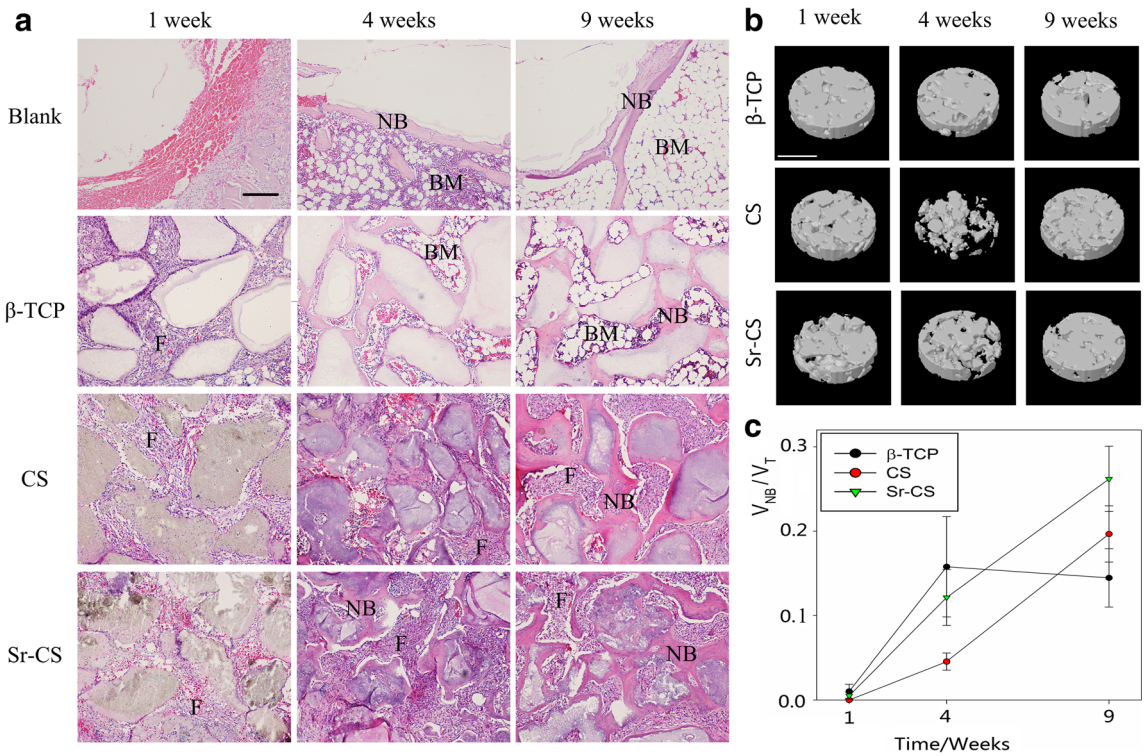

Fig. 3 Micro-CT and tissue section results. **a** H&E staining. New bone (*NB*) is stained *pink/pale pink*; bone marrow is marked with *BM* and fibrous tissues *F*. *Scale bar* 200 μm. **b** 3D reconstructions of the volume of interest (VOI) using AC=12.55 m^{-1} as the threshold value. *Scale bar* 1 mm. **c** Semi-quantitative image analysis results for H&E sections. Variation of new bone volume/tissue volume ratio (V_{NB}/T_V) with time; n=8

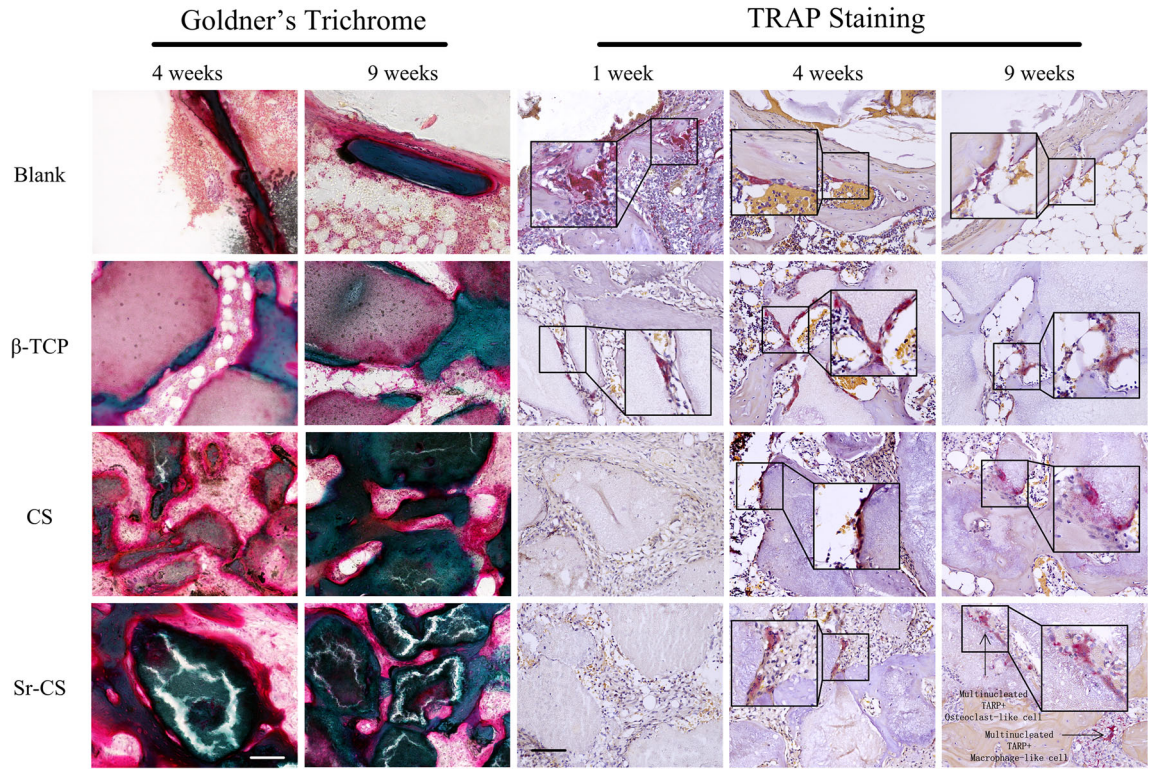

Fig. 4 Tissue section results. In Goldner's trichrome staining, new osteoid is stained *red*; calcified new bone is *dark green*. *Scale bar* 100 μm. In TRAP staining, TRAP-positive osteoclast-like cells (magnified view) were stained *red-purple*. The osteoclast-like cells are multinucleated, attached to the bone or implant surface and TRAP positive. While macrophage-like cells are also multinucleated, but in the centre of the bone marrow, and could be either TRAP positive or TRAP negative. None were found for CS and Sr-CS at 1 week. *Scale bar* 100 μm

Discussion

To begin, it is worth rehearsing the meaning of pH in the present context. It would seem that interfacial pH is the most significant aspect with respect to cells in contact with any surface: the normal condition is intimate conformity, and this and subsequent behaviour must be affected by the chemistry of that surface. This value cannot be ascertained because it depends on the interaction of cell membrane and that material and no physical probe is feasible. More broadly, the physiological background pH is a function, inter alia, of respiration and ventilation, establishing body- and organ-scale gradients affected by tissue type and perfusion rate. Tissue fluid and blood pH can be measured relatively easily and representatively, recognizing that these are 'local' in a general sense. Superimposed on those ordinary pH gradients in tissues will be the effects of implanted materials and be relevant down to the cellular scale. It is these local gradients that can be expected to dominate in the broader tissue response, directing and modulating behaviour within a region defined by the distance at which the perturbation becomes undetectable against the background state. The physical size of a probe means that while microenvironment pH measurements can be made, they are necessarily 'averaged' over a sample volume. We are mindful, therefore, that while we report and discuss μe-pH as if for point values, this is necessarily an approximation, but one that serves to dilute (rather than exaggerate) the apparent stimulus (i.e. departure from the norm) offered by an implanted material.

We have previously demonstrated that a material's fluid interfacial pH is appreciably different from that of the bulk medium in vitro [11] and that this increased pH was one of the factors which affected the performance of strontium-doped borosilicate [12]. However, the influence from beneficial ions released from biomaterial extraction in vitro has been widely reported, while the role of pH influenced by biodegradable systems has seldom been discussed. Here, increased pH stimulates osteogenic differentiation while inhibits osteoclast precursors proliferation and differentiation. On the one hand, the increased pH is supposed to provide an optimal condition for ALP activity (Supplementary Fig. 1) and to disrupt pre-osteoclasts to fuse into active multinucleated osteoclasts; on the other hand, pH below the physiological level stimulates TRAP-positive pre-osteoclasts fused together (Fig. 1e). Consistent with in vitro results, materials with higher μe-pH demonstrated better anabolic osteoid formation activity; at the same time, the catabolic activity of TRAP-positive cells was not detected under the same conditions in vivo (Fig. 4). These

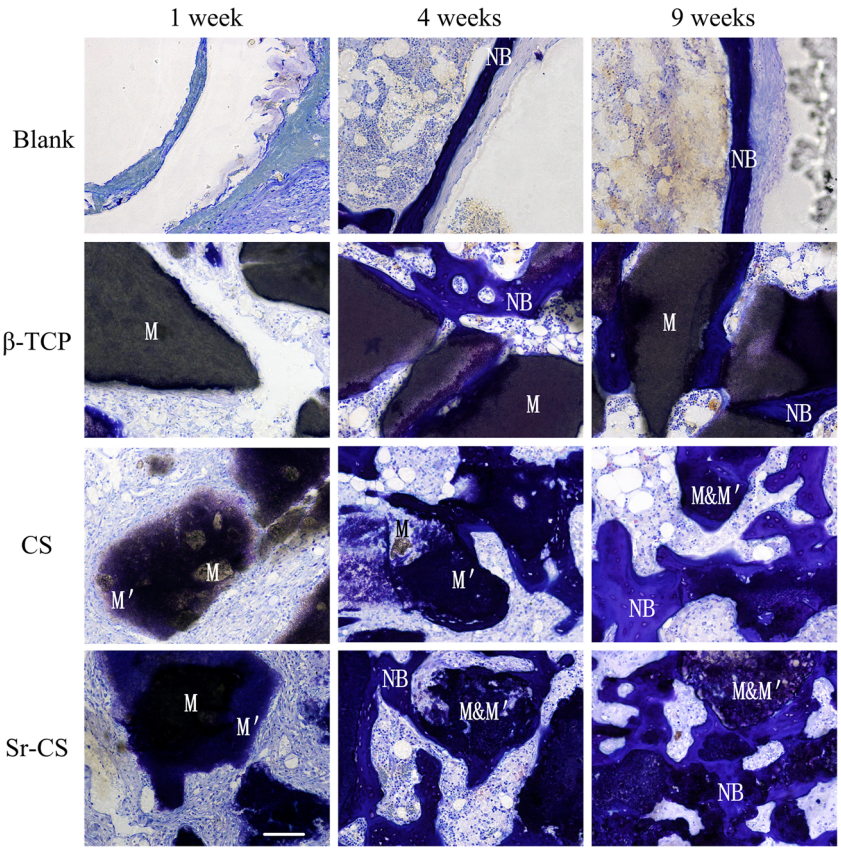

Fig. 5 Undecalcified tissue section results, toluidine blue staining. Implant materials (*M*) appear *black* or *gray*; new bone (*NB*) is stained *blue* (osteocyte lacunae can be clearly observed). 'Apatitic' intermediate layer (*M′*), lacking lacunae, found for CS and Sr-CS. *Scale bar* 100 μm

results suggest that imbalance in the conditions for remodeling osteoporotic bone may be ameliorated by adjusting the material to generate a weakly alkaline microenvironment. Equally, a weakly acid microenvironment should be avoided since it appears to stimulate osteoclast differentiation (Fig. 1d). Thus, specific designed alkaline biomaterials were employed, and the in vivo μe-pH of different implants were then monitored spatio-temporally.

Other studies [33] have also indicated that the extracellular acid-base equilibrium influences the function of bone cells and bone mineralization processes. Under lower pH conditions (pH 6.5~7.0), osteoclasts show a sharp increase in activity, though the optimal pH for osteoclast differentiation and proliferation has been said to be 7.0~7.5 [34]. Arnett reported that the resorption activity of cultured osteoclasts shows maximum stimulation when the pH is decreased to 6.9 [35]. Weak alkaline conditions (pH 7.4~7.8) in the extracellular medium stimulate osteoblasts' collagen gene expression, ALP activity and collagen secretion [36–38]. A comparatively high pH (pH>8.0) is essential for optimum activity of osteoblast alkaline phosphatase in vitro [39]. With the increase of pH, osteoclastic β-glucuronidase synthesis, together with osteoclast resorption activity, decreased [8]. In addition, hydroxyapatite solubility is also influenced by the local pH (i.e. pOH):

$$10Ca^{2+} + 6PO_4^{3-} + 2OH^- \leftrightarrow Ca_{10}(PO_4)_6(OH)_2$$

a higher pH shifting the equilibrium to the right and apparently stimulating the formation of the intermediate bioactive 'apatitic' layer and the mineralization process.

The immediate tissue response after implantation, as well as the complexity of the composition of the materials, means that it is impossible to calculate the theoretical in vivo μe-pH, making direct measurement essential. Here, the in vivo μe-pH was detected by microelectrode pH sensor, which provides a wide dynamic pH response and allows sensitive detection. It is a reliable detection technique which has been applied in the determination of the pH of skin [40], tumour [41], kidney [42] and other tissues. The minimum detection scope of the microelectrode was 1.3 mm, that is to say, the μe-pH values reported here apply to the region within 1.3 mm of the implantation site. As discussed above, it is nevertheless a relatively broad region which include blood, tissue fluid and extracellular matrix and must be influenced by both implant and tissue response. However, in order to provide a continuous monitoring of μe-pH, the development of better, protein-resistant pH microelectrodes, and especially ones capable of long-term implantation, would be valuable.

The initial stage (seconds to days) of implantation is probably one of the most important stages, if not the most important, as it influences ECM protein adsorption, cell attachment and proliferation, MSC differentiation and migration, cell function (mineralization) and ultimately the overall

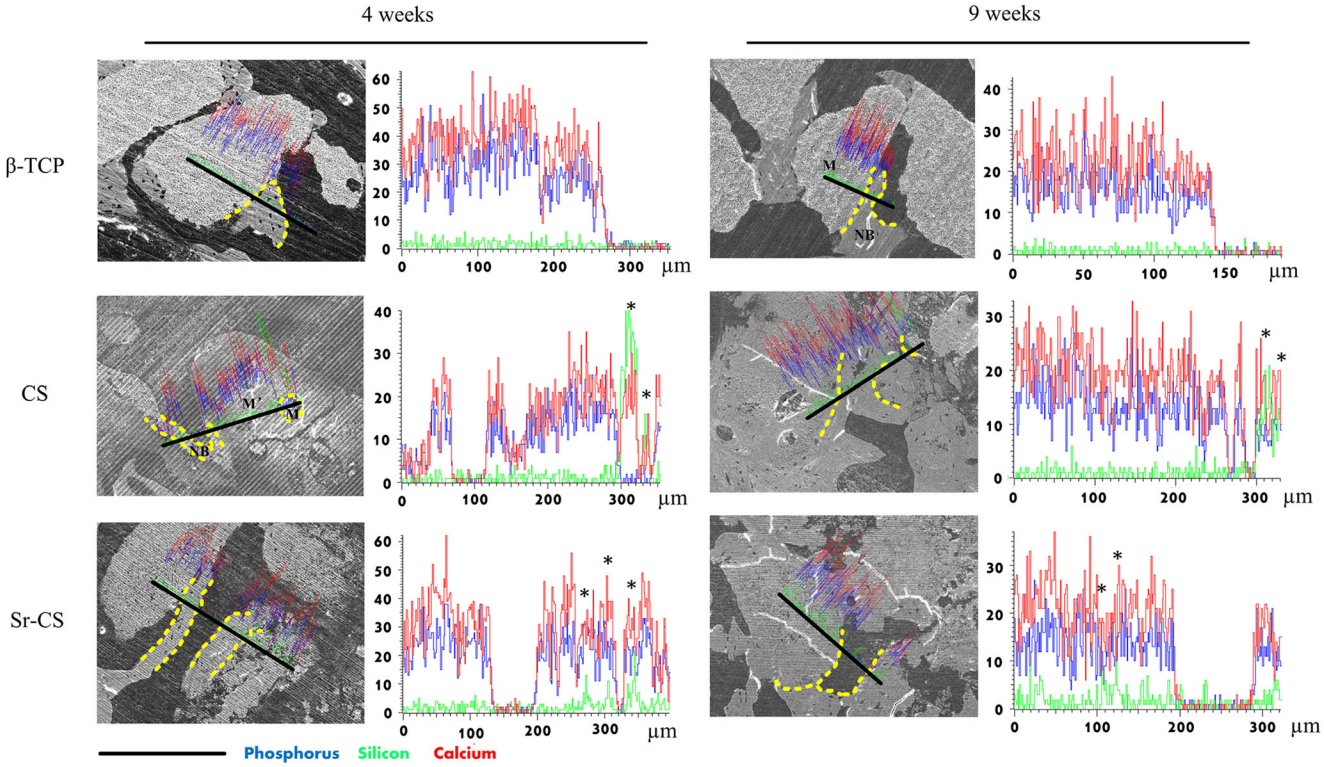

Fig. 6 Representative elemental line scans across material implantation sites, EDX scanning. *Black lines* indicate scan track; *red* indicates Ca; *blue* indicates P; *green* indicates Si;. Si-rich regions are marked with *asterisks*. The Ca-P-rich areas for CS and Sr-CS, without osteocyte lacunae, believed to be the intermediate layers. Boundaries between materials, intermediate layers and new bone are marked with *broken yellow lines*. *M* implant material, *NB* new bone, *M'*: 'apatitic' intermediate layer. *Scale bar* 300 μm

performance of the implant [43]. Here, significant differences in μe-pH in vivo between materials at this stage were found. Given the nature of the ions released in the degradation of the implant materials, the increase in μe-pH in the bone defect area was as expected and confined to the locality of the implant itself.

The host response to materials in the skeletal defect healing process also influences the μe-pH value. Chakkalakal et al. demonstrated that the pH of the surroundings of a demineralized bone matrix implantation in vivo went through a 'first decrease, then increase' process [26], with which our results are consistent (Fig. 2). However, the μe-pH decreasing process under the osteoporotic bone defect healing process may have been caused by both the loss of remaining material and the tissue inflammatory response. We therefore hypothesize that 'alkaline' materials engender a higher μe-pH in vivo and thus play a key role in the bone defect healing process under unbalanced osteoporotic bone remodeling conditions. However, alkaline μe-pH values higher than the normal tissue value inhibited the proliferation of oBMSCs (Fig. 1a). Also, in vivo experiments indicated that the inflammatory fibrous tissue still remained 9 weeks post-surgery in the higher μe-pH groups (CS and Sr-CS, Fig. 3). The optimal μe-pH for the best biomaterial performance in the osteoporotic condition, and how the higher pH condition may be utilized without invoking a prolonged inflammatory response, need to be ascertained.

It is also recognized that other variables, such as the release of factors beneficial to bone regrowth, may affect the performance of implants. Also, compared with the blank, implanted materials not only provide biochemical stimuli for tissue regeneration but also work as scaffolds for tissues to grow into. It is, however, impossible to design such materials differing in μe-pH but which are otherwise identical in all other properties and characteristics. We also recognize that μe-pH may be an intermediate variable: i.e. variation in μe-pH is generated by the implanted materials, which then in turn influences the overall behaviour of those materials (for example, degradation rate). Therefore, different materials could generate similar in vivo μe-pH from both their inherent pH effect and interaction with the host response. In particular, the μe-pH of an implant as a carrier may also influence the activity of the included pharmaceutical substances. Furthermore, the alkaline μe-pH created by interaction between implants and tissue may play an important role in balancing the pH perturbation at the inflammation region of inflammatory (e.g. LPS)-induced osteoporosis.

To summarize, a weakly alkaline μe-pH has positive effects on osteoblast differentiation and inhibits osteoclast

formation. The in vivo local pH microenvironment is the result of the combination of the implant surface with attached cells, tissue fluid and blood; the net effect of the material's degradation products and the specific tissue response. We found that μe-pH differs from that of the homogeneous peripheral blood and exhibits variations over time particular to each biodegradable material. Higher μe-pH is associated with better overall performance: greater new bone formation and a late response of TRAP-positive osteoclast-like cells, as well as an intermediate 'apatitic' layer. Therefore, alkaline biodegradable materials with a μe-pH higher than physiological condition is advocated for better regeneration of osteoporotic bone defect. In addition, the pH microelectrode is suitable for in vivo μe-pH detection, and μe-pH may be used as one of the indices for biomaterial evaluation to better guide the design of such materials, not only in particular for osteoporotic bone defect repair but also in any situation where osseointegration is required.

Acknowledgments This work was supported by grants from the National Natural Science Foundation of China (No. 51272274, 51372170), the Development of Strategic Emerging Industries of the Shenzhen Basic Research Project (No. JCYJ20120617120444409), the Shenzhen Peacock Program (No. 110811003586331), Shenzhen Key Laboratory of Marine Biomedical Materials, ZDS (No. Y20130401165820356) and Hong Kong General Research Fund (No. 172057/14).

Conflicts of interest None.

References

1. Johnell O, Kanis JA (2006) An estimate of the worldwide prevalence and disability associated with osteoporotic fractures. Osteoporos Int 17:1726–1733
2. Feng X, McDonald JM (2011) Disorders of bone remodeling. Annu Rev Pathol 6:121–145
3. Arcos D, Boccaccini AR, Bohner M, Diez-Perez A, Epple M, Gomez-Barrena E et al (2014) The relevance of biomaterials to the prevention and treatment of osteoporosis. Acta Biomater 10: 1793–1805
4. Delmas PD (2002) Treatment of postmenopausal osteoporosis. Lancet 359:2018–2026
5. Black DM, Cummings SR, Karpf DB, Cauley JA, Thompson DE, Nevitt MC et al (1996) Randomised trial of effect of alendronate on risk of fracture in women with existing vertebral fractures. Lancet 348:1535–1541
6. Bushinsky DA (2001) Acid–base imbalance and the skeleton. Eur J Nutr 40:238–244
7. Brandao-Burch A, Utting JC, Orriss IR, Arnett TR (2005) Acidosis inhibits bone formation by osteoblasts in vitro by preventing mineralization. Calcif Tissue Int 77:167–174
8. Bushinsky DA (1996) Metabolic alkalosis decreases bone calcium efflux by suppressing osteoclasts and stimulating osteoblasts. Am J Physiol 271:F216–F222
9. Kaunitz JD, Yamaguchi DT (2008) TNAP, TrAP, Ecto-purinergic signaling, and bone remodeling. J Cell Biochem 105:655–662
10. Harada M, Udagawa N, Fukasawa K, Hiraoka BY, Mogi M (1986) Inorganic pyrophosphatase activity of purified bovine pulp alkaline phosphatase at physiological pH. J Dent Res 65:125–127
11. Shen YH, Liu WC, Lin KL, Pan HB, Darvell BW, Peng SL et al (2011) Interfacial pH: a critical factor for osteoporotic bone regeneration. Langmuir 27:2701–2708
12. Shen YH, Liu WC, Wen CY, Pan HB, Wang T, Darvell BW et al (2012) Bone regeneration: importance of local pH-strontium-doped borosilicate scaffold. J Mater Chem 22:8662–8670
13. Hench LL (2006) The story of Bioglass (R). J Mater Sci-Mater Med 17:967–978
14. Zhang WB, Shen YH, Pan HB, Lin KL, Liu XG, Darvell BW et al (2011) Effects of strontium in modified biomaterials. Acta Biomater 7:800–808
15. Ciapetti G, Cenni E, Pratelli L, Pizzoferrato A (1993) In vitro evaluation of cell/biomaterial interaction by MTT assay. Biomaterials 14:359–364
16. Nilsson B, Korsgren O, Lambris JD, Ekdahl KN (2010) Can cells and biomaterials in therapeutic medicine be shielded from innate immune recognition? Trends Immunol 31:32–38
17. Gorbet MB, Sefton MV (2004) Biomaterial-associated thrombosis: roles of coagulation factors, complement, platelets and leukocytes. Biomaterials 25:5681–5703
18. Korostynska O, Arshak K, Gill E, Arshak A (2008) Review paper: materials and techniques for in vivo pH monitoring. IEEE Sensors J 8:20–28
19. Zhou DD (2008) Microelectrodes for in-vivo determination of pH. In: Zhang XJ, Ju HX, Wang J (eds) Electrochemical sensors, biosensors and their biomedical applications. Academic Press, USA, pp 261–305
20. Pandolfino JE, Ghosh S, Zhang Q, Heath M, Bombeck T, Kahrilas PJ (2006) Slimline vs. glass pH electrodes: what degree of accuracy should we expect? Aliment Pharmacol Ther 23:331–340
21. Ruan CM, Zeng KF, Grimes CA (2003) A mass-sensitive pH sensor based on a stimuli-responsive polymer. Anal Chim Acta 497: 123–131
22. Bock C, Sartoris FJ, Wittig RM, Portner HO (2001) Temperature-dependent pH regulation in stenothermal Antarctic and eurythermal temperate eelpout (Zoarcidae): an in-vivo NMR study. Polar Biol 24:869–874
23. Lee H, Akers W, Bhushan K, Bloch S, Sudlow G, Tang R et al (2011) Near-infrared pH-activatable fluorescent probes for imaging primary and metastatic breast tumors. Bioconjug Chem 22:777–784
24. Zhang XM, Lin YX, Gillies RJ (2010) Tumor pH and its measurement. J Nucl Med 51:1167–1170
25. Bartsch I, Willbold E, Rosenhahn B, Witte F (2014) Non-invasive pH determination adjacent to degradable biomaterials in vivo. Acta Biomater 10:34–39
26. Chakkalakal DA, Mashoof AA, Novak J, Strates BS, McGuire MH (1994) Mineralization and pH relationships in healing skeletal defects grafted with demineralized bone matrix. J Biomed Mater Res 28:1439–1443
27. Xu S, Lin K, Wang Z, Chang J, Wang L, Lu J et al (2008) Reconstruction of calvarial defect of rabbits using porous calcium silicate bioactive ceramics. Biomaterials 29:2588–2596
28. Zhu H, Guo ZK, Jiang XX, Li H, Wang XY, Yao HY et al (2010) A protocol for isolation and culture of mesenchymal stem cells from mouse compact bone. Nat Protoc 5:550–560
29. Lelovas PP, Xanthos TT, Thoma SE, Lyritis GP, Dontasi IA (2008) The laboratory rat as an animal model for osteoporosis research. Comp Med 58:424–430
30. Westendorf JJ (2008) Osteoporosis: methods and protocols. Humana Press, Totowa
31. An YH, Martin KL (2003) Handbook of histology methods for bone and cartilage. Humana Press, Totowa

32. Kadoya Y, al-Saffar N, Kobayashi A, Revell PA (1994) The expression of osteoclast markers on foreign body giant cells. Bone Miner 27:85–96
33. Kato K, Matsushita M (2014) Proton concentrations can be a major contributor to the modification of osteoclast and osteoblast differentiation, working independently of extracellular bicarbonate ions. J Bone Miner Metab 32:17–28
34. Shibutani T, Heersche JNM (1993) Effect of medium-pH on osteoclast activity and osteoclast formation in cultures of dispersed rabbit osteoclasts. J Bone Miner Res 8:331–336
35. Arnett T (2003) Regulation of bone cell function by acid–base balance. Proc Nutr Soc 62:511–520
36. Kohn DH, Sarmadi M, Helman JI, Krebsbach PH (2002) Effects of pH on human bone marrow stromal cells in vitro: implications for tissue engineering of bone. J Biomed Mater Res 60:292–299
37. Kaysinger KK, Ramp WK (1998) Extracellular pH modulates the activity of cultured human osteoblasts. J Cell Biochem 68:83–89
38. Arnett TR (2008) Extracellular pH regulates bone cell function. J Nutr 138:415S–418S
39. Ross MH, Ely JO, Archer JG (1951) Alkaline phosphatase activity and pH optima. J Biol Chem 192:561–568
40. Harrison DK, Walker WF (1979) Microelectrode measurement of skin pH in humans during ischemia, hypoxia and local hypothermia. J Physiol Lond 291:339–350
41. Jahde E, Rajewsky MF, Baumgartl H (1982) pH distributions in transplanted neural tumors and normal-tissues of BDIX rats as measured with pH microelectrodes. Cancer Res 42:1498–1504
42. Henderson RM, Bell PB, Cohen RD, Browning C, Iles RA (1986) Measurement of intracellular pH with microelectrodes in rat-kidney *in vivo*. Am J Physiol 250:F203–F209
43. Roach P, Eglin D, Rohde K, Perry CC (2007) Modern biomaterials: a review—bulk properties and implications of surface modifications. J Mater Sci Mater Med 18:1263–1277